Wetting and drying scheme for POM and its applications to San Francisco Bay

Y. Uchiyama
Port and Airport Research Institute, Yokosuka, Japan

ABSTRACT: A wetting and drying scheme (WDS) is developed to incorporate into a three-dimensional sigma-coordinate coastal ocean model with proposing an extended logarithmic profile within bed boundary layers to accurately simulate hydrodynamics in extremely shallow coastal seas. While WDS is simplistically formulated, it conserves water mass and has a good agreement with the analytical solution. The model is also applied to San Francisco Bay, California, which has considerably large intertidal areas, and is confirmed its accuracy by comparing observed data with the model-generated tidal elevations and currents.

1 INTRODUCTION

Estuarine intertidal mudflats and salt marshes have been recognized to play a significant role in marine environment and aquatic ecosystems. Efforts have been made to investigate hydrodynamics and associated sediment transport as well as chemical substances attached to the sediment particles on intertidal areas (e.g., Uchiyama et al., 2001; Talke and Stacey, 2003). A key factor dominating hydrodynamics on intertidal areas is wetting and drying processes since they affect suction of pore water in bed sediments influencing on sediment suspension, evaporation related to thermal and salinity environments of overlaying seawater, rapid movement of tidal currents resulting in formation of highly turbid "tidal bore" on the bed, and so on (Whitehouse et al., 2000). These facts imply that it is important to resolve micro-structure in the bed boundary layer in order to precisely assess sediment suspension and deposition.

In the present study, a wetting and drying scheme (WDS) is developed to incorporate into a three-dimensional σ-coordinate ocean model to simulate hydrodynamics in estuaries including intertidal areas such as mudflats and salt marshes (WD-POM). Attentions are paid particularly to mass conservation and hydrodynamic processes near the bed by adapting an extended logarithmic law so as to exactly predict vertical profiles of currents and turbulent structure in extremely shallow seas. WD-POM is at first applied to a run-up problem of non-linear long-waves on a sloping beach and is compared to the analytical solution. Next WD-POM is used to calculate tidal currents in San Francisco Bay, California, which has large intertidal area of about 200km^2 while the total surface area is 1240km^2. The accuracy of WD-POM is then confirmed by the harmonic analysis of the measured and the model-generated tidal currents.

2 METHODS

2.1 *Brief description of Princeton Ocean Model*

Princeton Ocean Model (POM) is based on a set of primitive equations consisting of the continuity equation, the 3D Reynolds-averaged Navier-Stokes equations, the heat and salinity transport equations, Mellor-Yamada level 2.5 turbulence closure model for vertical eddy mo-

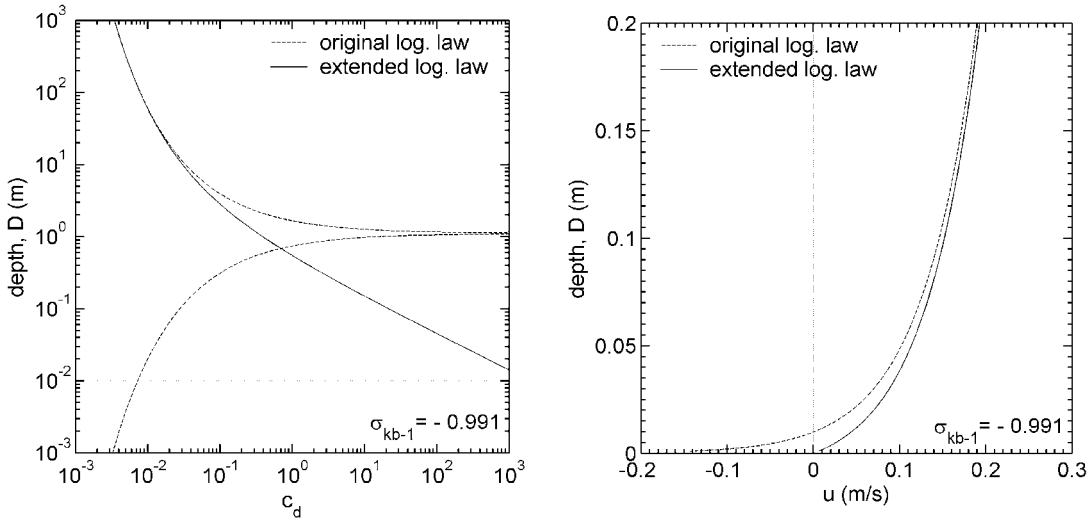

(a) vertical profile of C_d (b) vertical profile of velocity, U

Figure 1. Comparison between the original B.C. and the new B.C. using the extended logarithmic law

tion, and the Smagorinsky-type formulation for horizontal eddy diffusivity with the Boussinesq approximation and the hydrostatic assumption. The governing equations are transformed from the 3D Cartesian coordinate into the 2DH orthogonal curvilinear coordinate and the vertical σ coordinate to follow terrestrial topographies. The mode split technique is used in POM to solve the governing equations; it comprises the external mode to compute fast-moving 2DH surface gravity waves and the internal mode to estimate 3D vertical structure of currents, heat, salinity and turbulence. Several other techniques are also used to reduce computational times but they are not essential to the present study (for the detail, see Blumberg and Mellor, 1983).

2.2 *Wetting and drying scheme*

The WD-POM is configured for a pre-selected computational domain that contains both wet and dry grid cells. A land mask function (LMF) is created to mask out all land cells during model simulations. The LMF is assigned zero for all land cells and unity for all water cells. Technically no flux is allowed at the land-sea interface. The value of LMF at each grid cell is re-evaluated at each external time step based on a set of wetting/drying criteria. In the wetting and drying calculation presented here, the first step is to define three sub-depth scales, d_{cr}, d_{min}, and δ, prior to the simulations:

$$d_{cr} > d_{min} > \delta > 0. \tag{1}$$

The second step is to scan local water depth at each grid cell, $D_{i,j} = H_{i,j} + \eta_{i,j}$, where $H_{i,j}$ is a vertical level in z-coordinate below MSL (mean sea level) and $\eta_{i,j}$ is a water elevation above MSL in z-coordinate at a certain external time step. If $D_{i,j} \le d_{cr}$, where d_{cr} is a critical depth below which WDS is applied, the grid cell is regarded as potentially dry and WDS is immediately applied. In WDS three conditions are introduced to evaluate each of the potentially dry cell to be wet or dry by examining the four adjacent grid cells; 1) if the water elevations at all of the four cells are less than $\eta_{i,j}$, 2) if the water depths in all of the four cells are less than d_{cr}, or 3) if all of the four cells are effectively dry (LSM=0). If at least one of these three conditions is satisfied, the potentially dry grid is considered effectively dry and is subsequently removed from the computational domain; the LMF is set to be 0. Otherwise the grid cell is considered wet and remains in the simulation to be scanned again at the next time step; the LMF is held 1. When a cell becomes effectively dry, water elevation $\eta_{i,j}$ is stored in the memory and used in the next flooding. This procedure allows us to conserve the total water volume in the whole computational domain during the simulations.

The minimum depth, d_{min}, is used to avoid the zero depth because the σ-transformed primitive equations do not accept zero or negative water depths. When the horizontal grid spacing is sparse or the time step is set relatively large, the water surface may rapidly descend and be on or

below the seabed during an external time step. Whereas WDS itself guarantees mass conservation in the whole domain, it might sometimes fail if one employs no-zero d_{min}. However, the simulations become significantly robust with no-zero d_{min} particularly when an external time step is set larger or very sparse horizontal grid spacing is configured. In WD-POM, if the water depth D of a potentially dry cell is rapidly dewatered and becomes less than d_{min} during one single time step, the cell is considered effectively dry, the local water depth is held d_{min}, and LMF is set zero. Introducing d_{min} is likely equivalent to defining a thin sub-layer on the bed as used in Zheng et al. (2003; ZH03 hereafter), but the present method seems more flexible since users can control the performance of WD-POM by adjusting the value of d_{min}.

2.3 *Extended logarithmic law for bed boundary layer representation*

The last sub-depth scale in Eqn. (1), δ, is the most important one since it is used to retain the logarithmic velocity profile near the bed. In other words, δ is necessary to reflect microstructure within or above the bottom boundary layer and indispensable to correctly estimate bed shear stresses and resultant velocity profiles. In the original version of POM as well as the other versions used in the previous works by ZH03 and Xie et al. (2003), the boundary condition for the horizontal currents at the seabed is expresses as:

$$\frac{K_M}{D}\left(\frac{\partial U}{\partial \sigma}, \quad \frac{\partial V}{\partial \sigma}\right) = C_d\left[U^2 + V^2\right]^{1/2}(U, \quad V), \quad \sigma \to -1 \tag{2}$$

$$C_d = MAX\left[\frac{\kappa^2}{\left[\ln\{(1+\sigma_{kb-1})H/z_0\}\right]^2}, \quad 0.0025\right] \tag{3}$$

where K_M is vertical eddy diffusivity, U and V are horizontal 3D velocities, C_d is bed friction coefficient, κ is the von Karman constant, σ_{kb-1} is the lowest σ level for the horizontal current velocities, and z_0 is the roughness height usually being 1cm in estuaries. In the intertidal areas, variations in the water elevation η may be comparable to or greater than the water depth H relative to MSL, so that D must be used instead of H in Eqn. (3). In simulations of estuarine tidal currents, grid spacing may usually be logarithmically decreased towards the bed to resolve the bed boundary layer; the value of –0.991 for σ_{kb-1} is employed for the San Francisco Bay simulation. The extended logarithmic law represented by Eqn. (4) is therefore introduced to reproduce the structure of the bottom boundary layer properly.

$$C_d = \frac{\kappa^2}{\left[\ln\{(1+\sigma_{kb-1})D/z_0 + \delta/z_0\}\right]^2} \tag{4}$$

Equation (4) omits the pre-designated maximum value for C_d, which is originally set to avoid the boundary layer structure broken when depth is lowered to be extremely shallow, and introduces δ/z_0 in the denominator. This procedure is explained technically that it corresponds to elevating the grid system vertically at δ. In hydrodynamics no discrepancy is occurred because the bed shear stress used to the bottom boundary condition and the estimation of other fluxes are evaluated between the bed and the lowest grid points defined as $(1+\sigma_{kb-1})D/ z_0+\delta/z_0$. In practice the smaller value of δ we set, the more accurate estimation of the bed shear stresses can be achieved; the smallest value of $\delta=z_0$ is recommended as expressed in Eqn. (5).

$$C_d = \frac{\kappa^2}{\left[\ln\{(1+\sigma_{kb-1})D/z_0 + 1\}\right]^2} \tag{5}$$

Together with Eqn. (5), leaving the determination of l unchanged, the vertical eddy diffusivity must be slightly altered so that:

$$K_M = S_M q(l + \kappa\delta) = S_M q(l + \kappa z_0), \tag{6}$$

where S_M, q and l are respectively the stability function, the square root of TKE multiplied by 2, and the turbulent macro-scale. The final result seems equivalent to the 1D model for the oscil-

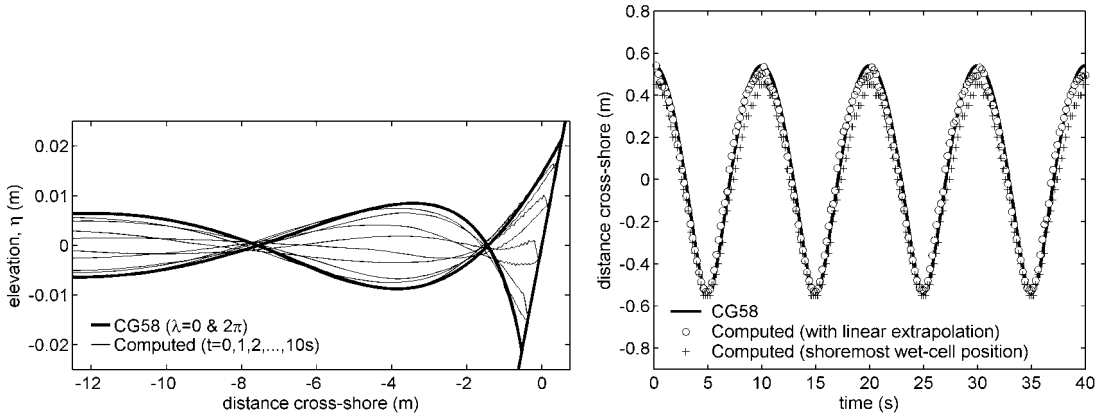

(a) superposition of water surface (b) shoreline positions

Figure 2. Comparison of the results from WD-POM and CG58.

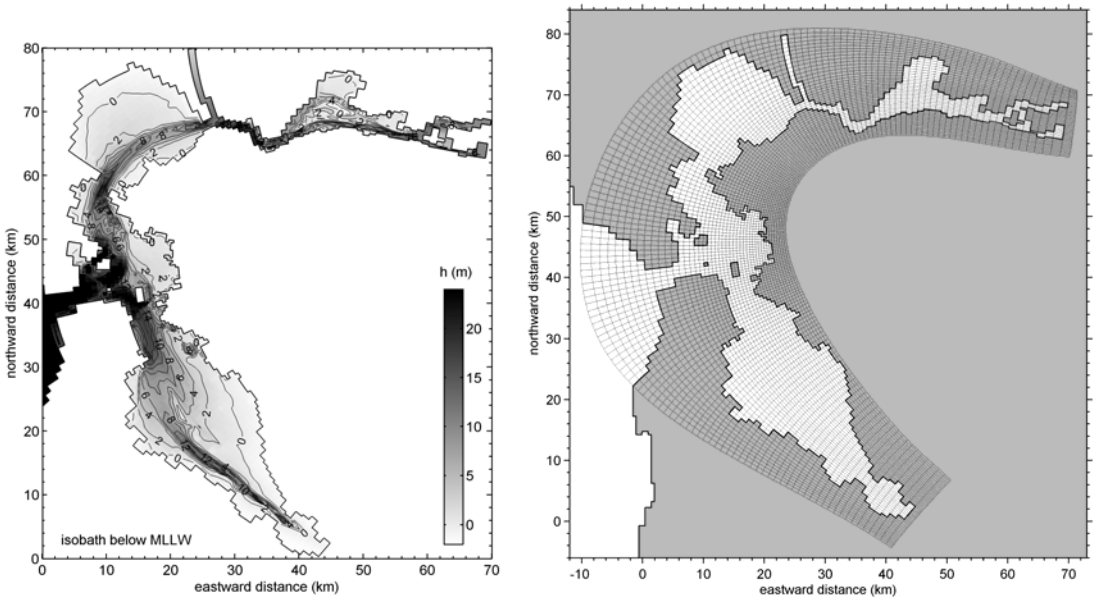

Figure 3. Bathymetric map of San Francisco Bay, California, USA (left) and the computational grid alignment using the horizontal orthogonal curvilinear transformation (right)

latory boundary layer proposed by Mellor (2002). As illustrated in Figure 1, the structure of the bottom boundary layer (C_d) based on the original logarithmic law is much different from that based on the extended log-law particularly if $\delta = z_0$ is employed and $(1+\sigma_{kb-1})D/\ z_0+\delta/z_0$ approaches z_0. Apparently the original log-law has remarkable error in estimation of C_d near the bed and the extended log-law is found to precisely replicate the structure of the bed boundary layer. Note that δ is not used in the σ-transformation, so that δ is independent of D and can be set zero if simulations do not include intertidal inundation and drainage.

3 RESULTS AND DISCUSSION

Whereas WDS presented here is formulated simplistically, it guarantees mass conservation and can control numerical robustness in accordance with the value of d_{min}, and replicates the benthic boundary layer precisely particularly when computations are carried out for estuaries that have extremely shallow or intertidal areas. The numerical solution derived from WD-POM is next compared to the analytical solution for run-up of non-linear long-waves on a sloping beach (Carrier and Greenspan, 1958; CG58 hereafter). Figure 2 (a) indicates superposition of water surfaces reproduced by the model at several phases and by CG58 at the phases of 0 and 2π. The model-generated water surfaces seem to have reasonable agreement with those by

Table 1. Four dominant components of harmonic constituents for tidal currents
(OBS: observed, MDL: model-predicted, DIF: difference between OBS and MDL)

		Major Axis (cm/s)			Orientation (°)			Phase Epoch (°)		
Locations		OBS	MDL	DIF	OBS	MDL	DIF	OBS	MDL	DIF
Richmond	M_2	75.8	68.6	−7.2	118.8	105.2	−13.6	176.4	170.8	−5.6
	S_2	21.6	19.3	−2.3	116.0	105.4	−10.6	172.8	168.1	−4.7
	K_1	23.3	21.7	−1.6	121.6	105.5	−16.1	161.8	157.9	−3.9
	O_1	16.7	14.0	−2.7	120.2	105.4	−14.8	155.0	148.7	−6.3
Oakland	M_2	52.5	48.6	−3.9	99.8	103.7	3.9	326.6	325.6	1.0
	S_2	14.6	16.7	1.9	102.0	103.4	1.4	318.1	318.2	0.1
	K_1	10.4	11.8	1.4	100.0	105.1	5.1	298.6	309.7	11.1
	O_1	4.5	6.0	1.5	110.7	106.8	−3.9	277.2	297.2	20.0

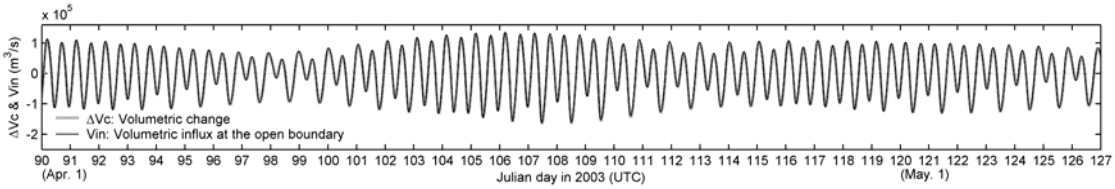

Figure 4. Volume influx at the open boundary, V_{in}, and volumetric change, ΔV_c.

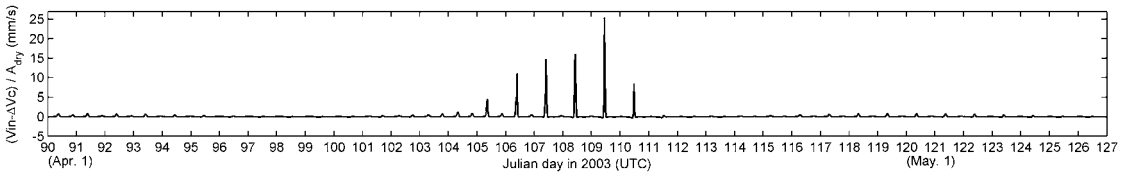

Figure 5. Errors in volume per unit area of dry cells, $(V_{\text{in}}-\Delta V_c)/A_{dry}$: A_{dry} is drained area.

CG58 although minor noises, that may be caused by reflected waves from the moving boundary, are produced near the shoreline, suggesting WD-POM is capable of simulating the wetting and drying accurately. Similar agreement is also found in the temporal variations in the shoreline positions calculated by the model and CG58 as shown in Figure 2 (b).

The model is next applied to San Francisco Bay (Figure 3), California, which has the surface area of about 1,240km^2 and is encompassed by intertidal mudflats of about 200km^2. South Bay is often described as "a tidally oscillating lagoon with density-driven exchanges with the northern reach", and North Bay including San Pablo Bay and Suisun Bay has huge influx from the Sacramento-San Joaquin drainage basin. The simulation is conducted for 40 days by solely imposing the astronomical tidal elevations on the open boundary condition off Golden Gate (west of the bay mouth). The scaling factors are set as d_{cr}=20cm, d_{min}=5cm, and δ=z_0=1cm, respectively. The model-generated water elevations and 3D horizontal velocities in the whole computational domain are decomposed into 17 dominant harmonic constituents and compared to the observed data as listed in Tables 1. It is validated that the model successfully reproduces propagation of surface gravity waves and a tidal currents observed by NOAA-NOS (2003) in San Francisco Bay. Mass conservation check is next performed as represented in Figures 4 and 5. The volume influx at the open boundary is almost equal to the volumetric change integrated for the whole computational domain, indicating that the water mass is basically conserved except during the spring tide. Although some spiky but minor errors are found during this period, it returns to have a value of about zero (i.e., no error is measured) immediately after the spring tide.

Instantaneous distributions of 2DH current vectors, water surface elevations, and dry cells at two phases during the spring tide, at ebbing and high slack phases, are displayed in Figure 6. The current fields are realistic and agree with the results by Cheng et al. (1993); the water surface rises and descends to inundate and drain out intertidal areas fringing the bay and strong currents are formed along the deeper channel.

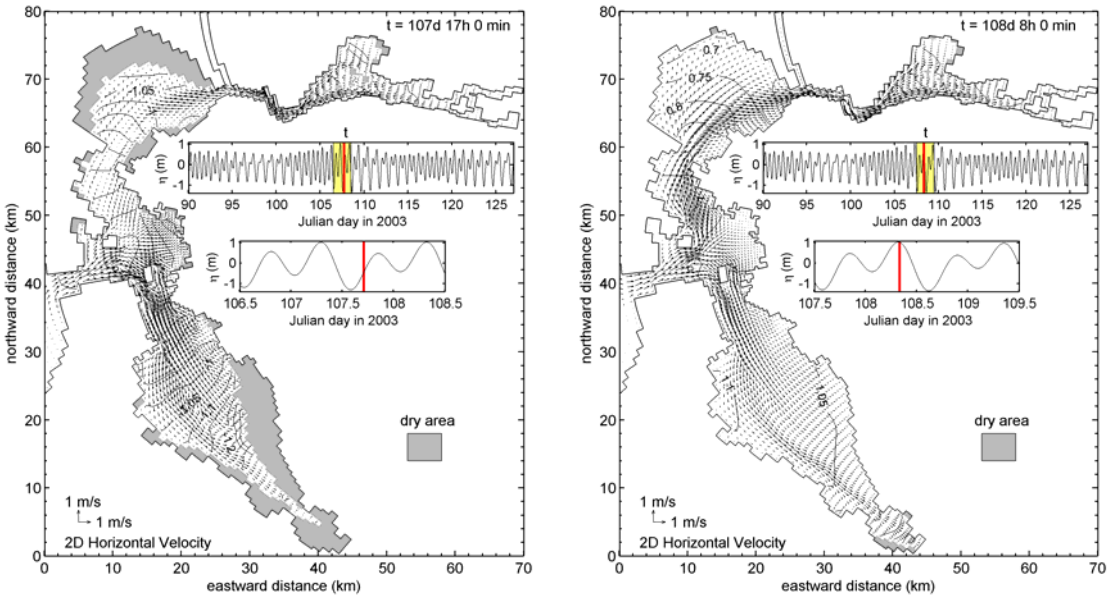

Figure 6. Distributions of 2DH current velocities, water elevations, and dry cells at ebbing phase (left) and high slack phase (right) during spring tide

4 CONCLUDING REMARKS

A wetting and drying scheme for a three-dimensional terrain-following coastal ocean model is developed by considering mass conservation and computational robustness. An extended logarithmic law for intertidal simulations is proposed to precisely reproduce the structure of bed boundary layer particularly on intertidal areas. The model performance is validated by comparing to the CG58 theory and the observed tidal current data in San Francisco Bay to demonstrate a good agreement. A residual current field, a vorticity budget, mixing processes around the interfaces between intertidal and deeper areas, and detailed hydrodynamics induced by wetting and drying, etc. should be investigated in the future.

REFERENCES

Blumberg, A.F. and Mellor, G.L., 1983. Diagnostic and prognostic numerical circulation studies of the South Atlantic Bight, *J. Geophys. Res.*, 88: 4579-4593.

Carrier, G.F. and Greenspan, H.P., 1958. Water waves of finite amplitude of a sloping beach, *J. Fluid Mech.*, 4: 97-109.

Cheng, R.T., Casulli, V. and Gartner, J.W., 1993. Tidal, residual, intertidal mudflat (TRIM) model and its application to San Francisco Bay, California, *Estuarine, Coastal and Shelf Sci.*, 36: 235-280.

Mellor, G.L., 2002. Oscillatory Boundary Layers, *J. Phys. Oceanogr.*, 32: 3075-3088.

National Ocean Service, National Oceanic and Atmospheric Administration (NOS-NOAA), 2003. http://www.co-ops.nos.noaa.gov/.

Talke, S.A. and Stacey, M.T., 2003. The influence of oceanic swell on flows over an estuarine intertidal mudflat in San Francisco Bay, *Estuarine, Coastal and Shelf Sci.*, 58: 541-554.

Uchiyama, Y., Kuriyama, Y. and Katoh, K., 2001. Suspended sediment and morphological response on Banzu tidal flat, Japan, *Proc.4th Int'l Conf. Coastal Dynamics*, ASCE: 1038-1047.

Whitehouse, R.J.S., Soulsby, R.L., Roberts, W. and Mitchener,H.J., 2000. Intertidal Processes, In: *Dynamics of estuarine muds*, Thomas Telford, London, UK: 163-168.

Xie, L., Pietrafesa, L.J. and Peng, M., 2003. Incorporation of a mass-conserving inundation scheme into a three dimensional storm surge model, *J. Coastal Res.*, 1-17.

Zheng, L., Chen, C. and Liu, H., 2003. A modeling study of the Satilla River Estuary, Georgia. I: Flooding-drying process and water exchange over the salt marsh-estuary-shelf complex, *Estuaries*, 26 (3): 651-669.